Research Square

Preprints are preliminary reports that have not undergone peer review.
They should not be considered conclusive, used to inform clinical practice,
or referenced by the media as validated information.

Understanding molecular mechanisms behind the anti-inflammatory effects of Machilus macrantha (Gulmavu) in the arachidonic acid metabolic pathway by network pharmacological approach

NABARUN MUKHOPADHYAY
National Institute of Pharmaceutical Education and Research
SIBU SEN
National Institute of Pharmaceutical Education and Research
ASHISH KUMAR
National Institute of Pharmaceutical Education and Research
RUJUTA SANDBHOR
National Institute of Pharmaceutical Education and Research
AMOL G DIKUNDWAR
National Institute of Pharmaceutical Education and Research
VENKATA RAO KAKI
kvenkata.rao@niperhyd.ac.in

National Institute of Pharmaceutical Education and Research

Research Article

Keywords: Molecular mechanisms, anti-inflammatory, arachidonic acid metabolism, Machilus macrantha, Network Pharmacology

Posted Date: October 25th, 2024

DOI: https://doi.org/10.21203/rs.3.rs-5288974/v1

License: This work is licensed under a Creative Commons Attribution 4.0 International License.
Read Full License

Additional Declarations: No competing interests reported.

Abstract

Background

Inflammation is a critical defense mechanism that mainly occurs in the human body through arachidonic acid metabolism and is needed to maintain a healthy life, but uncontrolled inflammation leads to several diseases like asthma, osteoarthritis, etc. *Machilus macrantha* is an important Indian medicinal plant that is traditionally used as an anti-inflammatory, anti-rheumatic agent but has yet to be explored much. Hence, the present study has been undertaken to elucidate the molecular mechanisms underlying its anti-inflammatory activity in the arachidonic acid metabolic pathway by using network pharmacology and molecular modelling studies.

Results

Several free online tools and databases like SEA, Swiss target prediction, OMIM, GeneCards, Venny 2.1.0, and STRING were utilized to predict, compile, and filter the anti-inflammatory targets, and a total of 23 targets were obtained throughout the process. Further, by using the topology parameters (degree, betweenness, and closeness) in Cytoscape 3.10.0 software, a total of five hub nodes or genes named PTGS2, NFκβ1, MAPK1, CYP2C8, and CYP2C9 were identified which is mainly associated with arachidonic acid metabolism. KEGG and GO analyses were performed by using the SRplot tool, and it was observed that arachidonic acid metabolism emerged as the top pathway with the lowest *P*-value and highest fold enrichment. The tissue enrichment studies of the hub genes were also performed using the Human eFP Browser. Finally, a ligand-target-pathway interaction network was created, which proved that the phytoconstituents of *M. macrantha* interact with multiple molecular targets of arachidonic acid metabolism and showed anti-inflammatory activity. Molecular docking and molecular dynamics simulation studies proved that a total of three ligands named machigline, machiline, and quercetin exhibited moderate to good binding efficacies toward the hub genes, and machigline and quercetin showed stability in the binding cavity.

Conclusion

From the present study, it can be concluded that the phytocompounds of *M. macrantha* have significant interactions with anti-inflammatory targets specifically on arachidonic acid metabolism, hence the same can act as an important source for developing novel anti-inflammatory agents.

Keywords:

Molecular mechanisms, anti-inflammatory, arachidonic acid metabolism, *Machilus macrantha*, Network Pharmacology

1 Background

Inflammation is a complex defense mechanism triggered by several mediators like pro-inflammatory cytokines, immune cells, etc, which help to heal the human body by acting against intrinsic and extrinsic stimuli and maintaining cellular homeostasis [1]. Usually, inflammatory conditions are characterized by the following conditions: swelling, redness, pain, and fever. The process of inflammation is generally classified into two types based on the onset of duration: chronic and acute inflammation; acute inflammation helps to keep our body healthy, but several diseases like cancer, Alzheimer's disease, obesity, osteoarthritis, etc. are associated with chronic inflammation [2]. Arachidonic acid metabolism is majorly responsible for the initiation and progression of inflammatory pathways. It further activates lipoxygenase (LOX) and cyclooxygenase (COX) enzymes to produce prostaglandins and leukotrienes [3]. Generally, COX has two isoforms, and LOX has four isoforms named COX-1, COX-2, 5-LOX, 12-LOX, 8-LOX, and 15-LOX, respectively, and some of the prominent by-products released through these enzymes are 5-HPETE, LTB4 and LTE4, etc [4, 5]. Hence, by inhibiting these enzymes, safe and efficacious anti-inflammatory agents can be developed. Among all isoforms of COX and LOX enzymes, COX-2 and 5-LOX were mainly explored in this direction, and selective 5-LOX and COX-2 inhibitors were designed and utilized [6, 7]. Even, for getting better therapeutic activity and reducing the risk of gastrointestinal disorders, dual COX-LOX inhibitors were also developed [8]. Natural products play a major role in the development of novel and safer anti-inflammatory agents by showing prominent inhibition towards COX and LOX enzymes [8]. Different classes of natural products, like saponins, terpenoids, alkaloids, phenolics, coumarins, etc., were explored in this direction [9, 10].

Machilus macrantha, commonly known as gulmavu, picchilataru was available in the Indian states of Maharashtra, Karnataka, Bihar, and Kerala and majorly cultivated in the western ghats region [11]. Gaind and Baveja have carried out phytochemical investigations of roots. The alcoholic extract of the limed roots indicated the presence of alkaloids. Machiline was the major alkaloid separated from the alcoholic extract, which was later shown to be identical to dl-coclaurine, an alkaloid also reported in *Cocculus laurifolius* and *Machilus kusanoi* [12, 13]. Baveja, S.K. *et al*. also isolated β-sitosterol and two alkaloids from the root [14]. Two new alkaloids, namely machigline, and atheroline were also isolated [15]. Traditionally, the bark of this plant was used for treating rheumatoid arthritis, tuberculosis, and asthma. Egg-white is mixed with powdered bark and applied locally to the affected part in the form of a poultice act as an anti-inflammatory and anti-rheumatic agent by Hallakki Gowda tribes of western ghats region, Karnataka, India [15, 16]. The decoction of powdered bark is made with honey and is taken to treat asthma and rheumatism [16]. This plant has several important pharmacological uses. Tatiya AU *et al.* demonstrated the antioxidant activity of this plant using various *in vitro* models. [17]. Y.A. Kulkarni *et al*. tried to validate the ethnopharmacological claims of the anti-inflammatory activity of *M. macrantha* bark, and for this purpose, different extracts have been prepared from this plant by using different organic solvents like petroleum ether, chloroform, methanol, and water and tested for anti-inflammatory activity. From this study, it was observed that the aqueous extract and petroleum ether extract showed significant anti-inflammatory activity [18].

Network pharmacology, first stated by Hopkins, is a unique field of science that integrates network science, bioinformatics, multidimensional pharmacology, etc. [19, 20]. This approach eventually establishes a link between the ligands and diseases, which helps in the development of novel drugs [20]. Nowadays, the network

pharmacological approach has become popular in natural product-based drug discovery, and several researches have been done in this direction. Das J. *et al.* conducted a network pharmacology-based investigation on the *Phyllanthus fraternus* medicinal plant and identified the possible main genes responsible for its pharmacological activity and also identified the phytoconstituents involved in the interactions [21]. Sasikumar NSD *et al.* collected information regarding some important and widely used dietary phytochemicals, and by performing network pharmacological analysis of the same for Parkinson's disease, the main molecular targets were identified, ligands were screened, and the possible molecular pathways were also predicted [22].

In the present study, a network pharmacological approach was utilized to understand the molecular mechanisms behind the anti-inflammatory activity of *M. macrantha*, specifically focusing on arachidonic acid metabolism. As per our knowledge, this kind of study was not conducted earlier on this particular medicinal plant, and hence, it was a novel study, and may help the researchers to perform further *in-vitro* and *in-vivo* pharmacological studies.

2 Methods

2.1 Selection of predicted targets of the phytoconstituents of *M. macrantha*

By thorough exploration of different research articles collected from online databases like ScienceDirect, Pubmed, Google Scholar, Wiley online library, etc., and with the help of IMPPAT database [23], a total of five phytoconstituents named Quercetin (Flavonoid), atheroline (Isoaporphine alkaloid), machiline (benzylisoquinoline alkaloid), β-sitosterol (Steroid) and Machigline (Aporphine alkaloid) were isolated and characterized to date from this plant. The potential targets for these phytoconstituents were predicted by incorporating the "Canonical SMILES" of the same in different databases like SEA, Swiss Target Prediction [24, 25]. Further, the final targets were selected by filtering and combining the targets obtained from the two databases. The entire study protocol was depicted in Fig. 1.

2.2 Prediction and selection of anti-inflammatory targets using by the phytoconstituents of *M. macrantha*

The specific anti-inflammatory targets were predicted by entering different keywords like "inflammation" and "anti-inflammatory" in free online databases like OMIM, and GeneCards [26, 27]. Further, the targets obtained from these two databases were combined to get the main and major anti-inflammatory targets. The same and the predicted targets for the phytoconstituents of *M. macrantha* were added in Venny 2.1.0 [28], and the intersection of both exhibited the major anti-inflammatory targets of the active constituents of *M. macrantha.*

2.3 Gene-gene interaction (GGI) network construction using phytoconstituents of *M. macrantha*

For constructing the protein-protein interaction (PPI) network, the above-mentioned anti-inflammatory targets were entered into the STRING database [29]. The required parameters were correctly set to get a robust network ("Homo sapiens" as an organism, minimum interaction threshold score (high confidence =0.7, for other parameters the default values were only kept). Further, the created network was incorporated into the Cytoscape 3.10.0 software, and the topological parameters (Betweenness, closeness, and degree) were employed by using "cytoHubba" plugin for each node of the prepared network. The greater the values of these parameters of any node, the more important the position of that particular node will be in the network. Further, the average values

of all three parameters were calculated, and the specific targets with more values than the corresponding average were selected as the final anti-inflammatory targets of the phytoconstituents of *M. macrantha.*

2.4 Gene ontology and pathway enrichment analysis of the final anti-inflammatory targets

The final anti-inflammatory targets were taken and incorporated in the SRplot tool [30], and gene ontology (GO) and pathway enrichment analyses (KEGG) were performed (Species- Homo sapiens and P <0.05). From the KEGG database, the final pathways were obtained with their particular enrichment scores. The GO analysis was majorly focused on three parameters: GO cellular component (CC), GO Biological process (BP), and GO molecular function (MF), and also the enrichment GO term.

2.5 Tissue enrichment of the final anti-inflammatory targets

The entire human body expression distribution map was obtained by using the Human eFP Browser [31], and the distribution of expression of the final anti-inflammatory targets will be known by this process.

2.6 Preparation of phytoconstituents (ligand)-target-pathway interaction network

The respective excel files were prepared for botanicals, botanicals with bioactives, botanical bioactives with targets, and pathways with genes and imported in Cytoscape 3.10.0. The constituents or ligands were selected as the source node and the genes were selected as the target node and further, the network was visualized after selecting the proper layout (Degree sorted circle layout).

2.7 Molecular docking studies of the phytoconstituents of *M. macrantha*

Molecular docking studies were performed using Schrodinger Drug Design suite 2022.4.

2.7.1 Ligand preparation

LigPrep module was utilized for the preparation of ligands to be docked. The structure of the ligands was generated using ChemDraw ultra software [32]. Ligand preparation was carried out to convert molecules into energy minimized 3D formats. For this purpose, the molecules were ionized at physiological pH and generated the possible tautomeric states. During the process, specific chirality of molecules was retained, and minimization was done using OPLS4 (Optimized Potential for Liquid Simulations) [33, 34, 35].

2.7.2 Protein preparation and Grid generation

The X-ray crystal structure of proteins Cytochrome P450 2C8 (PDB id: 2NNH), Extracellular signal regulated kinase 2 (PDB id: 3W55), Sodium voltage channel gated alpha subunit (PDB id: 5K7K), Cyclooxygenase 2 (PDB id: 5KIR), Nuclear factor kB (PDB id: 8TQD) was obtained from the RCSB protein data bank [36]. Protein preparation wizard tool was utilized for the preparation of proteins. The protocol of protein preparation included addition of polar explicit hydrogen atoms, creation of di sulfide bonds and deletion of water molecules till 3Å from heteroatoms. Additionally, the missing side chains and loops in proteins were filled using prime [37]. Restrainement of hydrogen atoms was performed using force field OPLS4 [38].

Glide grid generation tool was used for the generation of grid on the prepared protein. The grid was generated centroid of the co-crystal ligand present in the proteins keeping the grid box size 20Å [39].

2.7.3 Molecular docking and Binding free energy calculation

Molecular docking of prepared ligands on the generated grid was carried out using Glide module. Docking was performed in Standard Precision (SP) mode for the robustness and output was set as pose viewer file including receptor [40].

Physics based approach molecular mechanics energy combined with Generalized Born and surface area continuum solvation (MM-GBSA) was used for the calculation of binding free energy of ligand with the macromolecule. Prime MM-GBSA module was utilized for this purpose. The binding energy was calculated using force field OPLS4 and solvation model VSGB as optimized implicit solvent model [41].

2.8 Molecular dynamics simulation

In order to assess the stability of macromolecule-ligand complex stability in human body, a simulated environment was created computationally and then analyzed the stability of complex. Desmond software integrated in Schrodinger Drug design suite was utilized for running the molecular dynamics simulation. Simulation was performed on two complexes 5KIR-Machigline and 8TQD-Quercetin. For 8TQD-Quercetin complex membrane setup was done prior to system building. Initially system was built using system builder panel by placing them into orthorhombic shape box (Size 10x10x10 Å and angles between each side 90°) and explicit TIP3P (transferable intermolecular potential 3 point) water model was used for solvation [42]. The built system was minimized and then added ions for neutralization and 0.15M NaCl salt to stabilize the net charge on the system. These protocols were utilized for creating environment similar to human body. The system for both 5KIR-Machigline and 8TQD- Quercetin contained 56184 and 34682 atoms respectively. Molecular dynamics simulation was run for 100ns with recording intervals of 100ps and recorded 1000 frames during the simulation. NPT (Constant number atoms N, 1.01325 bar pressure and 300K temperature) ensemble was used for constant temperature and pressure condition that was managed by Nose-Hover Chain thermostat and Martyna-Tobias-Klein barostat respectively [43, 44].

2.9 *In silico* ADME scrutinization

The pharmacokinetics of small molecule is governed by absorption, distribution, metabolism and excretion (ADME). These studies are important because they control the activity of the small molecules inside human body. The drug likeness of the ligand was analyzed by Lipinski's Rule of five and Jorgensen Rule of 3. The ADME and drug likeness study was carried out using Qikprop module [45].

3 Results

3.1 Prediction of the potential targets of the phytoconstituents of *M. macrantha*

By putting the "Canonical SMILES" of the five constituents named quercetin, atheroline, machigline, *β*-sitosterol, and machiline found in different parts of *M. macrantha* plant in different online databases like Swiss Target Prediction, SEA, the potential targets were predicted and merged further.

3.2 Identification of the main anti-inflammatory targets for the phytoconstituents of *M. macrantha*

The inflammation-related targets were collected from databases like GeneCards, OMIM, etc., and the predicted targets of the phytoconstituents were incorporated in Venny 2.1.0. A total of 23 main anti-inflammatory targets were obtained after de-duplication (Fig. 2).

3.3 Establishment of PPI (protein-protein interaction) network targeting inflammation using phytoconstituents of *M. macrantha*

The above mentioned 23 anti-inflammatory targets were first added to the STRING database, and the PPI interactions were obtained (Fig. 3) for the same targets. The TSV file of the created network was downloaded and further incorporated into the Cytoscape 3.10.0 software. In this PPI network, 23 nodes and 40 edges were there, with an average betweenness, degree, and closeness of 9.81, 4.44, and 21.55, respectively (Table 1). Each node participating in the interactions was denoted with a circle, and the circle's area became larger with increasing degree values; the thickness of the circle's border increased with increasing betweenness values, and circles got a dark colour with increasing values of closeness (Fig. 4). Five nodes or targets were found to have more than average values, which indicates their crucial position in the created network. These are the main targets of *M. macrantha,* which is responsible for its anti-inflammatory activity. The five targets named PTGS2, NFκβ1, MAPK1, CYP2C8, and CYP2C9 (Fig. 5) were further evaluated, and it was observed that PTGS2, CYP2C8, and CYP2C9 played an important role in the progression of arachidonic acid metabolism where PTGS2 is mainly responsible for the synthesis of prostaglandins and CYP2C8 and CYP2C9 generates ω-hydroxylated HETEs, particularly 20-HETE which act as pro-inflammatory mediators. Finally, MAPK1 and NFκβ1 genes are usually activated by arachidonic acid metabolism and are involved in inflammation.

3.4 GO and KEGG enrichment analysis of the anti-inflammatory targets

SRplot tool was utilized for performing GO and KEGG enrichment analysis, where 2,044 GO entries with P <0.05 were selected, including 1,826 biological processes, 127 molecular functions, and 91 cellular components. In Fig. 6, it was observed that the cellular components mainly included caveola, plasma membrane raft, and membrane raft; whereas in molecular functions included iron ion binding, aromatase activity, and heme binding are included; and biological processes majorly included arachidonic acid metabolic process, long-chain biosynthetic process, olefinic compound metabolic process, long-chain fatty acid metabolic process, etc.

A total of 10 KEGG pathways were selected, which may be correlated with the anti-inflammatory targets of *M. macrantha*, and the enrichment bubble plot for each selected pathway is mentioned in Fig. 7. Based on the degree of enrichment, the targets were arranged and are higher with more values. The colour of the bubbles represented the P-value, and it became redder with decreasing the same, and significant enrichment will be achieved. The pathways with more fold enrichment values included arachidonic acid metabolism, serotonergic synapse, etc. It was observed that the arachidonic acid metabolism pathway (Fig. 8) exhibited the lowest P-value and highest fold enrichment values.

3.5 Tissue enrichment of the selected anti-inflammatory targets

From the whole human body expression distribution map, it was observed that the gene expressions were not the same throughout the body. The levels of the main anti-inflammatory genes, or targets named PTGS2, NFκβ1, MAPK1, CYP2C8, and CYP2C9, were analyzed in the digestive, immune, and skeletal systems (Fig. 9). PTGS2

is highly expressed in the omental adipose tissues of the digestive, immune, and skeletal systems, whereas NFκβ1 and MAPK1 were mainly expressed in β-lymphocytes and bone marrow. The expression of CYP2C9 and CYP2C8 was highest in the liver.

3.6 Construction of ligand-target-pathway interaction network

A specific ligand-target-pathway interaction network (Fig. 10) was constructed using Cytoscape 3.10.0 software, and it consists of phytoconstituents, pathways, and target proteins. In this network, 29 nodes and 81 edges were there, and the selected five compounds interacted with 13 proteins by association with the enriched top 10 pathways.

3.7 Molecular docking studies of the phytocompounds obtained from *M. macrantha*

Relative orientation of molecules obtained from *M. macrantha* and macromolecules was predicted during molecular docking simulation. All the hit molecules were found to be interacting in binding cavity of the target protein in similar manner as standard molecules. The binding pose (Orientation and conformation) of molecules was extracted in 3D and 2D view and analysed the interacting amino acid during docking studies. Binding free energy score drew the information about stability of hit ligands and standard in complex with macromolecule.

Molecular docking study of phytocompounds and standard with the Cytochrome P450 2C8 (PDB ID: 2NNH) showed that although Machigline was found to be having less dock score (-6.72 kcal/mol) than that of standard Montelukast (-8.17 kcal/mol), it was better hit out of all the molecules. With the analysis of ligand binding free energy of both Machigline and Montelukast in complex with macromolecule it was inferred that Machigline was less stabilized in the cavity.

In the molecular docking of phytocompounds with Extracellular signal regulated Kinase 2, ERK2 (PDB ID: 3W55) Quercetin turned out be having more binding affinity (Dock score -8.09 kcal/mol) with the macromolecule than standard Ulixertinib (Dock score -7.76 kcal/mol). The ligand binding free energy analysis revealed that Ulixertinib was better stabilized than Quercetin. The ligand binding free energy of both Quercetin and Ulixertinib was found to be -59.19 kcal/mol and -70.63 kcal/mol respectively.

Machiline was predicted as best hit out of all the molecules during docking with alpha subunit of sodium voltage channel (PDB ID: 5K7K). The hit molecule Machiline was observed to be having better affinity with the macromolecule than standard Fluvastatin. The dock scores of Machiline and Fluvastatin was found to be -8.73 kcal/mol and -6.84 kcal/mol respectively. The ligand binding free energy of hit molecule Machiline and standard Fluvastatin was almost equal with scores -56.19 kcal/mol and -58.78 kcal/mol respectively.

Docking with the COX-2 enzyme (PDB ID: 5KIR) and phytocompounds predicted Machigline as best hit among all the phytocompounds. The binding affinity of hit Machigline (Dock score -8.54 kcal/mol) was observed to be lower than the standard Celecoxib (Dock score -11.40 kcal/mol). The ligand binding free energy also of Machigline was found to be less than Celecoxib confirming that Machigline was not as stabilized as Celecoxib. The binding free energy of both Machigline and Celecoxib was found to be -49.92 kcal/mol and -91.41 kcal/mol respectively.

Docking study of phytocompounds with the target Nuclear factor kB (PDB ID: 8TQD) elicited that Quercetin was having highest binding affinity with the macromolecule among all other, even higher than standard Imatinib. The dock score of both Quercetin and Imatinib was found to be -5.234 kcal/mol and -3.30 kcal/mol respectively confirming the better binding of Quercetin with the target. Contrary to binding affinity the ligand binding energy of Quercetin was lower than that of Imatinib with the scores -34.06 kcal/mol and -54.83 kcal/mol respectively.

In Fig. 11 and Table 2, 2D and 3D docking poses of the ligands and their specific binding interactions has been depicted.

3.8 Molecular dynamics simulation

Macromolecule-ligand complex stability was analyzed in terms of RMSD (root mean square deviation) and RMSF (root mean square fluctuations). The structural and dynamic behavior of ligand-macromolecule complex in simulated environment was analyzed throughout 100ns dynamics simulation (Fig. 12 and Fig. 13).

In the protein-ligand RMSD plot of 5KIR-Machigline it was observed that both ligand and protein were stable throughout simulation. The RMSD of both protein and ligand was found to be 2.00Å and 1.75Å respectively. The protein-RMSF plot depicted that during the simulation run there were no significant conformational changes observed in protein chain during ligand association. Apart from this it was also observed that amino acid set 90-92, 305-315, 490-500 were forming major interactions. From the protein-ligand contacts it was observed that most of the interaction were hydrophobic with the amino acid residues Arg120, Val349, Trp387, Phe518, Val523 and Ala527 having interaction fraction more than 50%. Hydrogen bonding interactions were observed with the amino acid residues Tyr385 and Ser530. Ligand-Protein contacts analysis showed that Arg120, Tyr385, Arg513 and Ser530 were major interacting residues. Arg120 interacted with the aromatic rings of ligand forming Pi-cation bonding occupying 34% and 38% time of total simulation time. Tyr385 interacted with the hydroxyl group of the ligand forming hydrogen bonding and water bridges occupying 11% and 20% of total simulation time. Dioxole ring interacted with the amino acid residue Arg513 forming water bridges. Carbonyl function group of ligand formed two interactions with Ser530 namely hydrogen bonding and water bridges occupying 17% and 28% of total simulation time.

The Protein-Ligand RMSD plot of 8TQD-quercetin showed that the protein was stable during the simulation and no structural conformational changes were observed. The ligand RMSD was slightly higher and during time frame 65-75 ns it diffused from the protein cavity, rest of the time it was stable in the protein cavity. The protein and ligand RMSD was found to be 2.25Å and 21Å respectively. The protein RMSF plot depicted that amino acid residues 140-140 fluctuated most during the simulation with average RMSF for the protein 3.0Å. During the simulation it was observed that amino acid sets 15-30, 70-80, 100-110, 200-207 were forming interaction with the ligand. Protein-Ligand contacts showed that amino acids Tyr59, Cys61, Glu62, His143 and Lys146 were contributing to major interaction by forming hydrophobic, hydrogen bonding and water bridges. Ligand-Protein contacts of 8TQD-Quercetin showed that a strong intramolecular H-bond was forming in the ligand. Tyr59 showed pi-pi interaction with the chromenone moiety occupying 21% time of total simulation run. His143 formed pi-pi as well as salt bridge with the ligand with occupancy of 8% and 6% of total simulation

time. Lys146 interacted with chromenone moiety of the ligand forming two pi-cation interactions occupying 8 and 6% of total simulation time.

4 Discussion

Inflammation is a complex pathophysiological process that helps to keep the human body healthy. It is mainly regulated by arachidonic acid metabolism, which is further progressed by COX and LOX enzymes [46]. Hence, inhibition of both of the enzymes is a major approach toward the development of novel anti-inflammatory agents. In this direction, natural products, specifically plant-based natural products, can be utilized as a lead, and several types of research have also been done.

Machilus macrantha is an ethnopharmacologically important medicinal plant which is having numerous important pharmacological uses like anti-asthmatic, anti-inflammatory, anti-rheumatic etc [15]. But, till now, this plant has not been explored much by the scientific community. Hence, the same has been selected for the current study to determine the potential targets and the molecular mechanisms responsible for its anti-inflammatory activity (focusing on arachidonic acid metabolism).

In this study, the anti-inflammatory targets for the phytoconstituents named quercetin, atheroline, machigline, *β*-sitosterol, and machiline of *M. macrantha* were mined using different free online tools like SEA, Swiss Target Prediction, etc. Further, a total of 23 targets were obtained after filtering and combining all predicted targets. Thereafter, the PPI network was constructed utilizing the STRING database and the same has 23 nodes and 40 edges. The Cytoscape 3.10.0 software helped us to get the main hub genes or nodes (based on topology factors like degree, closeness, and betweenness) of this particular network and named PTGS2, NFκβ1, MAPK1, CYP2C8, and CYP2C9. These five genes were mainly responsible for the molecular interactions with the obtained phytoconstituents and played a major role in the activation and progression of the arachidonic acid metabolism process. Through KEGG enrichment analysis, it was found that arachidonic acid metabolism is the prevalent pathway with the highest fold enrichment and lowest *P*-value. Hence, it can be concluded that the phytoconstituents of this plant may show anti-inflammatory activity by inhibition of arachidonic acid metabolism. The expression levels of the hub genes in the skeletal, digestive, and immune systems were evaluated, and it was observed that these genes were mainly expressed in omental adipose tissues, *β*-lymphocytes, bone marrow, and liver. Finally, a specific ligand-target-pathway interaction network was formed with 29 nodes and 81 edges, and it showed interactions with multiple proteins associated with the pathways obtained from KEGG enrichment analysis.

Molecular docking studies showed that out of five ligands taken, quercetin, machigline, and machiline showed good to moderate binding affinity (based on docking score and calculated binding energy) against the main anti-inflammatory targets. Quercetin showed good binding affinity against Extracellular signal regulated kinases 2 (ERK2), which is comparable to ulixertinib, but in the case of nuclear factor kB, it showed less binding affinity compared to imatinib. Machigline showed moderate binding affinity against both cytochrome P450 2C8 protein and COX-2 enzyme compared to the respective standards named montelukast and celecoxib.

Molecular simulation exhibited that the two ligands named machigline and quercetin are quite stable in the binding cavities of the top two proteins named 5KIR and 8TQD denoted for COX-2 enzyme and Nuclear factor

kB (based on RMSD and RMSF). From these studies, it is quite evident that quercetin, machigline, and machiline may be responsible for the multi-target interactions of *M. macrantha* in arachidonic acid metabolism.

The above-mentioned three ligands named, quercetin, machigline, and machiline were within the permissible limits of pharmacokinetic parameters (Table 3) except for quercetin which has poor Caco2 cell permeability.

5 Conclusion

M. macrantha, also known as gulmavu, acts on the arachidonic acid metabolism pathway for treating inflammation by interacting with multiple molecular targets, and this may help the researchers towards the selection of particular anti-inflammatory targets while exploring this medicinal plant. Our current study also depicts the multi-target mechanisms of the phytoconstituents of *M. macrantha* to treat and prevent inflammation. Hence, it can be concluded from the present study that, *M. macrantha* may be utilized as a source for developing safe, efficacious anti-inflammatory agents. However, further *in-vitro* and *in-vivo* pharmacological studies need to be performed to get more information about its therapeutic efficacies.

Ethics approval and consent to participate

Not applicable.

Funding

None.

List of abbreviations

COX	Cyclooxygenase
LOX	Lipoxygenase
GGI	Gene-gene interaction
KEGG	Kyoto Encyclopaedia of Genes and Genomes
GO	Gene Ontology
PPI	Protein-protein interaction
STRING	Search tool for the retrieval of interacting genes
BP	Biological Process
MF	Molecular Function
CC	Cellular Component

PDB	Protein Data Bank
RMSD	Root-mean-square deviation
RMSF	Root-mean-square fluctuation
MD	Molecular Dynamics
OPLS4	Optimized Potentials for Liquid Simulations 4

References

1. Das K, Buchholz N (2019) Benign prostate hyperplasia and nutrition. Clinical Nutrition ESPEN 33:5–11. https://doi.org/10.1016/j.clnesp.2019.07.015
2. Murata M (2018) Inflammation and cancer. Environmental Health and Preventive Medicine 23:50. https://doi.org/10.1186/s12199-018-0740-1
3. Meshram MA, Bhise UO, Makhal PN, Kaki VR (2021) Synthetically-tailored and nature-derived dual COX-2/5-LOX inhibitors: structural aspects and SAR. Eur J Med Chem 225:113804. https://doi.org/10.1016/j.ejmech.2021.113804
4. Maxis K, Delalandre A, Pelletier JM, Pelletier JP, Duval N, Lajeunesse D (2006) The Shunt from the Cyclooxygenase to Lipoxygenase Pathway in Human Osteoarthritic Subchondral Osteoblasts Is Linked with a Variable Expression of the 5 Lipoxygenase-Activating Protein. Arthritis Res Ther R181. https://doi.org/10.1186/ar2092
5. Kutil Z, Temml V, Maghradze D, Pribylova M, Dvorakova M, Schuster D, Vanek T, Landa P (2014) Impact of Wines and Wine Constituents on Cyclooxygenase-1, Cyclooxygenase-2, and 5-lipoxygenase Catalytic Activity. Mediators Inflamm 178931. https://doi.org/10.1155/2014/178931
6. Yunus MHM, Nordin A, Kamal H (2020) Pathophysiological perspective of osteoarthritis. Medicina 56:1–13. https://doi.org/10.3390/medicina56110614
7. Nikalje PG, Tiwari SV, Sangshetti JN, Damale MD (2018) Ultrasound-mediated synthesis, biological evaluation, docking and *in- vivo* acute oral toxicity study of novel indolin-2-one coupled pyrimidine derivatives. Res Chem Intermed 44:3031–3059. https://doi.org/10.1007/s11164-018-3292-5
8. Mukhopadhyay N, Shukla A, Makhal PN, Kaki VR (2023) Natural product-driven dual COX-LOX inhibitors: Overview of recent studies on the development of novel anti-inflammatory agents. Heliyon 9:e14569. https://doi.org/10.1016/j.heliyon.2023.e14569 .
9. Ambati GG, Jachak SM (2020) Natural product inhibitors of cyclooxygenase (COX) enzyme: a review on current status and future perspective. Curr Med Chem 27:1–28. https://doi.org/10.2174/0929867327666200602131100
10. Sinha S, Doble M, Manju SL (2019) 5-Lipoxygenase as a drug target: a review on trends in inhibitors structural design, SAR and mechanism-based approach. Bioorg Med Chem 27:3745–3759. https://doi.org/10.1016/j.bmc.2019.06.040
11. http://www.biotik.org/india/species/ (website accessed on 23.07.2024)

12. Gaind KN, Baveja SK (1960) Investigation of *Machilus macrantha* Nees. II- Pharmacological action and chemical constitution of machiline. J Am Pharm Assoc Sci 49:663-665. https://doi.org/10.1002/jps.3030491010
13. Tomita M, Yang TH, Gaind KN, Baveja SK (1963) The structure of machiline, an alkaloid of *Machilus macrantha* Nees. Yakugaku Zasshi 83:218-220. https://doi.org/10.1248/yakushi1947.83.2_218
14. Baveja SK, Garg ML, Joneja MP (1968) Investigation of *Machilus macrantha* Nees. Part III. Ind J Pharm 30:11-13.
15. Tatiya AU, Saluja AK (2021) Further studies on membrane stabilizing, anti-inflammatory and FCA induced arthritic activity of various fractions of bark of *Machilus macrantha* in rats. Rev Bras Farmacogn 21(6):1052-1064. https://doi.org/10.1590/s0102-695x2011005000152
16. Harsha VH, Hebbar SS, Hegde GR, Shripathi V (2002) Ethnomedical knowledge of plants used by Kunabi Tribe of Karnataka in India. Fitoterapia 73(4):281-287.
17. Tatiya AU, Saluja AK (2008) Studies on Physico-chemical properties and antioxidant activity of mucilage polysaccharides from *Machilus macrantha* bark. J Res Educ Indian Med 1-6.
18. Kulkarni YA, Gokhale SB, Veeranjaneyulu A, Surana SJ, Tatiya AU (2009) Effect of *Persea macrantha* against acute inflammation and adjuvant-induced arthritis in rats, Pharm Biol 47(4):304–308. https://doi.org/10.1080/13880200902748437
19. Hopkins AL (2008) Network pharmacology: the next paradigm in drug discovery. *Nat Chem Biol* 4(114):682–690. https://doi.org/10.1038/nchembio.118
20. Liu CS, Xia T, Luo Z Y, Wu YY, Hu YN, Chen FL, Tang QF, Tan XM (2021) Network pharmacology and pharmacokinetics integrated strategy to investigate the pharmacological mechanism of Xianglian pill on ulcerative colitis. Phytomedicine 82:153458. https://doi.org/10.1016/j.phymed.2020.153458
21. Das J, Somabattini RA, Chhabra N, Roy PP, Islam R, Dhaked DK, Nanjappan SK (2023) Network pharmacology and bioinformatics based investigation of *Phyllanthus fraternus*: herb-drug interaction study. J Biomol Struct Dyn 1-15. https://doi.org/10.1080/07391102.2023.2291167
22. Sasikumar NDS, Thiruselvam P, Sundararajan V, Ravindran R, Gunasekaran S, Madathil D, Kaliamurthi S, Peslherbe GH, Selvaraj G, Sudhakaran SL (2024) Insights into dietary phytochemicals targeting Parkinson's disease key genes and pathways: A network pharmacology approach. Comput Biol Med 172:108195. https://doi.org/10.1016/j.compbiomed.2024.108195
23. https://cb.imsc.res.in/imppat/ (website accessed on 20.07.2024)
24. https://sea.bkslab.org/ (website accessed in 15.07.2024)
25. https://www.swisstargetprediction.ch/ (website accessed on 17.07.2024)
26. https://www.omim.org/ (website accessed on 17.07.2024)
27. https://www.genecards.org/ (website accessed on 20.07.2024)
28. https://bioinfogp.cnb.csic.es/tools/venny/ (website accessed on 20.07.2024)
29. https://string-db.org/ (website accessed on 17.07.2024)
30. https://www.bioinformatics.com.cn/basic_local_go_pathway_enrichment_analysis_122_en (website accessed on 20.07.2024)
31. https://bar.utoronto.ca/efp_human/cgi-bin/efpWeb.cgi (website accessed on 17.07.2024)

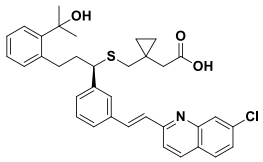
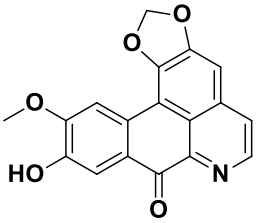
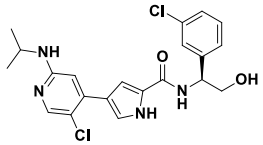
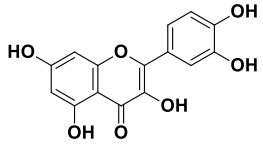
32. Machiraju PK, Yedla P, Gubbala SP, Bohari T, Jaleel KVA, Shili X, Patel R, Chittireddy VRR, Boppana K, Jagarlapudi SARP, Neamati N, Syed R, Amanchy R (2019) Identification, synthesis and evaluation of CSF1R inhibitors using fragment-based drug design. Comput Biol Chem 80:374-383. https://doi.org/10.1016/j.compbiolchem.2019.04.015
33. Shaikh AS, Sethi A, Makhal PN, Rathi B, Kaki VR (2023) Quest for selective MMP9 inhibitors: a computational approach. J Biomol Struct Dyn 41(24):15053-15066. https://doi.org/10.1080/07391102.2023.2186710
34. Manasa B, Manandhar S, Hari G, Priya K, Kumar B H, Pai KSR (2021) Virtual structure-based docking, WaterMap, and molecular dynamics guided identification of the potential natural compounds as inhibitors of protein-tyrosine phosphatase 1B. J Mol Struct 1226:129396. https://doi.org/10.1016/j.molstruc.2020.129396
35. Manual U. LigPrep 3.6.
36. RCSB Protein Data Bank. https://www.rcsb.org/ v
37. Kumar A, Rai S, Rathi E, Agarwal P, Kini SG (2021) Pharmacophore-guided fragment-based design of novel mammalian target of rapamycin inhibitors: extra precision docking, fingerprint-based 2D and atom-based 3D-QSAR modelling. J Biomol Struct Dyn 39(4):1155-1173. https://doi.org/10.1080/07391102.2020.1726816
38. Kawatkar S, Wang H, Czerminski R, Joseph MD (2009) Virtual fragment screening: An exploration of various docking and scoring protocols for fragments using Glide. J Comput Aided Mol Des 23(8):527-539. https://doi.org/10.1007/s10822-009-9281-4
39. Zhang XY, Li W, Wang J, Li N, Cheng Ms, Koike K (2019) Protein tyrosine phosphatase 1B inhibitory activities of ursane-type triterpenes from Chinese raspberry, fruits of *Rubus chingii*. Chin J Nat Med 17(1):15-21. https://doi.org/10.1016/s1875-5364(19)30004-4
40. Hosen SMZ, Kabir MSH, Hasanat A, Chowdhury TA, Chakrabarty N, Sarker SK, Habib MR, Dash R (2016) Docking and ADME/T analysis of silibinin as a potential inhibitor of EGFR kinase for ovarian cancer therapy. J Appl Pharm Sci 6(08):001-005. https://doi.org/10.7324/japs.2016.60801
41. Ramesh P, Veerappapillai S (2022) Management of RET-Positive Non-Small Cell Lung. 27(5):1590. https://doi.org/10.3390/molecules27051590
42. Saeed M, Shoaib A, Tasleem M, Alabdallah NM, Alam MJ, Asmar ZE, Jamal QMS, Bardakci F, Alqahtani SS, Ansari IA, Badraoui R (2021) Assessment of antidiabetic activity of the shikonin by allosteric inhibition of protein-tyrosine phosphatase 1b (Ptp1b) using state of art: An *in silico* and *in vitro* tactics. Molecules 26(13):3996. https://doi.org/10.3390/molecules26133996
43. Rajagopal K, Varakumar P, Aparna B, Byran G, Jupudi S (2021) Identification of some novel oxazine substituted 9-anilinoacridines as SARS-CoV-2 inhibitors for COVID-19 by molecular docking, free energy calculation and molecular dynamics studies. J Biomol Struct Dyn 39(15):5551-5562. https://doi.org/10.1080/07391102.2020.1798285
44. D. E. Shaw Research. Desmond Version 3.0 Tutorial. 2011;(April).
45. Pascoini AL, Federico LB, Arêas ALF, Verde BA, Freitas PG, Camps I (2019) *In silico* development of new acetylcholinesterase inhibitors. J Biomol Struct Dyn 37(4):1007-1021. https://doi.org/10.1080/07391102.2018.1447513

46. Bei Wang, Lujin Wu, Jing Chen, Lingli Dong, Chen Chen, Zheng Wen, Jiong Hu, Ingrid Fleming, Dao Wen Wang (2021) Metabolism pathways of arachidonic acids: mechanisms and potential therapeutic targets. Signal Transduction and Targeted Therapy, 6:94. https://doi.org/10.1038/s41392-020-00443-w

Table 1 Topology parameters of main anti-inflammatory targets of the active constituents of *M. macrantha*

Target	Degree	Betweenness	Closeness
PTGS2	10	160	13.33
NFKB1	6	72.5	11.08
MAPK1	5	48	10.58
CYP2C8	7	28	11.16
CYP2C9	7	28	11.16

Table 2 Interaction pattern of hit and standard molecules with the proteins

S.No	Molecule	H-bond	Halogen bond	Pi-Pi interaction	Pi-cation interaction	Hydrophobic interaction
			2NNH			
1.	Montelukast 	Asn217	Pro427			Ile102, Ile106, Phe201, Phe205, Leu208, Val362, Val366, Phe428, Ile434, Ala436
2.	Machigline 	Gly98	Thr386			Ile113, Ile213, Pro367, Ile476
			3W55			
1.	Ulixertinib 	Asp106, Met108, Asp111, Ser153	Lys114			Ile31, Val39, Ile84, Leu107, Tyr113, Leu156
2.	Quercetin 	Asp106, Met108, Asp111, Asn154, Cys166, Asp167				Ile31, Tyr35, Val39, Leu107, Leu156
			5K7K			
1.	Fluvastatin	Trp120, Arg433				Phe100, Ile112, Val113, Phe114, Leu208, Leu362, Leu366

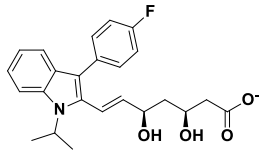
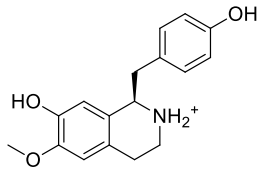
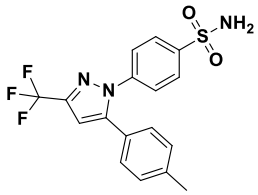
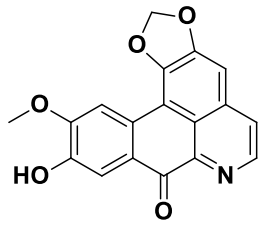
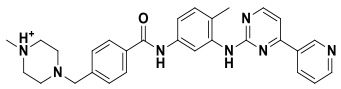
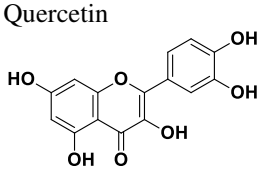
					
2.	Machiline	Thr301, Ser365			Val113, Leu361, Leu362, Leu366
					
	5KIR				
1.	Celecoxib	Gln192, Leu352, Arg513, Phe518			Met113, Val116, Tyr348, Val349, Leu359, Met521, Val523, Ala527
					
2.	Machigline	Ser530		Arg120	Val116, Tyr348,Val349, Leu352, Tyr355, Leu359, Met522, Val523, Ala527
					
	8TQD				
1.	Imatinib	Tyr59			Val60, Cys61, Val144, Ala244
					
2.	Quercetin	Val144	Tyr59		
					

Table 3 Pharmacokinetic profiling of the ligand molecules

Molecule	Mol.Wt.	log o/w	% human oral absorption	Human oral absorption	SASA	QPlogHERG	QPlog KHSA	QPPCac	QPPMD	Ro' 5	Ro'3
Quercetin	302.24	0.35	51.48	2	517.69	-5.078	-0.346	18.029	6.446	0	1
Machiline	285.34	2.10	79.30	3	544.86	-5.615	0.098	172.34	81.82	0	0
Machigline	321.28	1.917	89.57	3	503.87	-4.324	-0.128	744.612	359.68	0	0
β-sitosterol	414.71	7.52	100	1	759.03	-4.542	2.035	3381.95	1846.36	1	1
Atheroline	28.01	-0.18	88.33	3	154.59	-1.633	-1.397	3088.92	1674.07	0	0

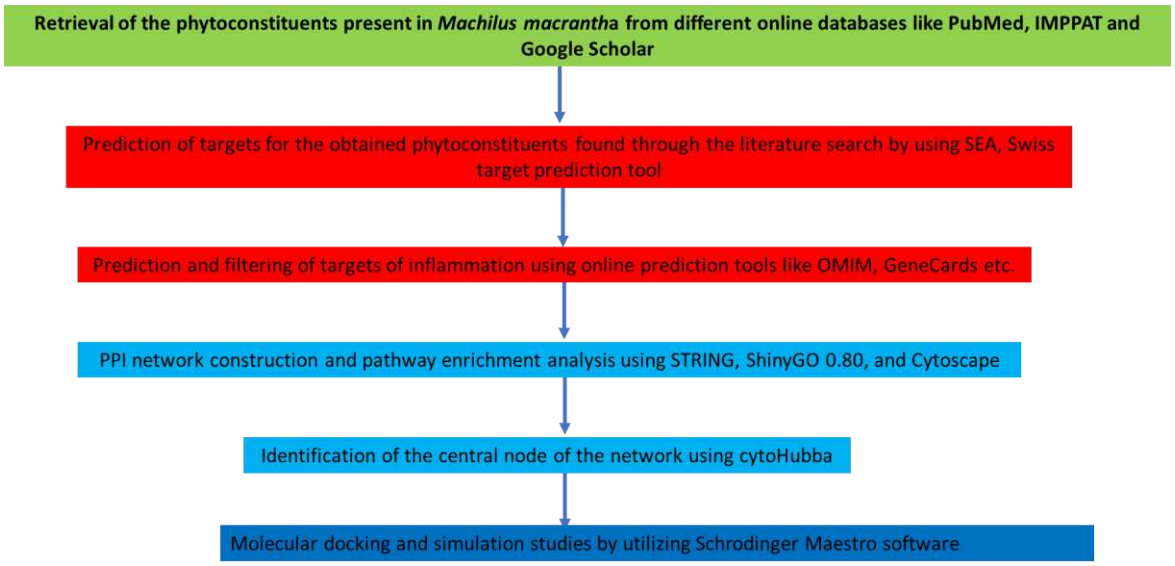


Fig. 1 Work flow of the study protocol

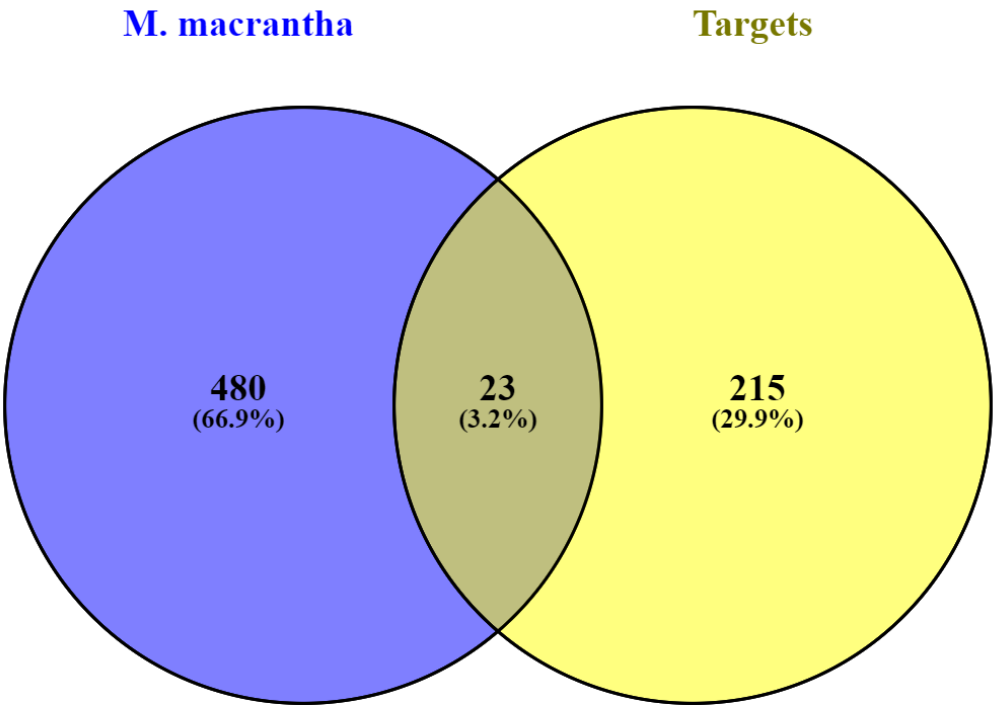


Fig. 2 Venn diagram (intersection denotes the major anti-inflammatory targets)

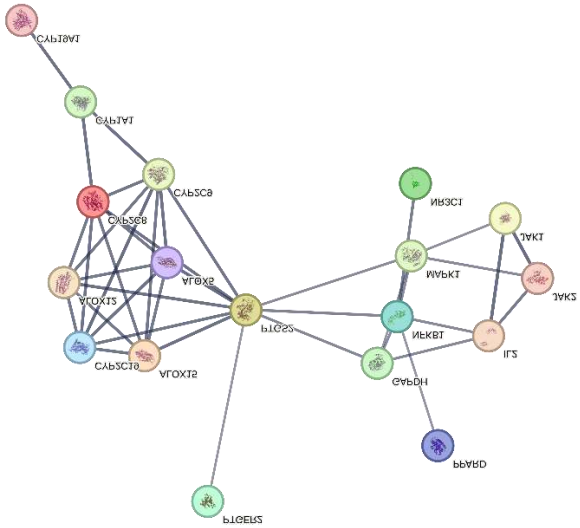


Fig. 3 PPI interaction diagram

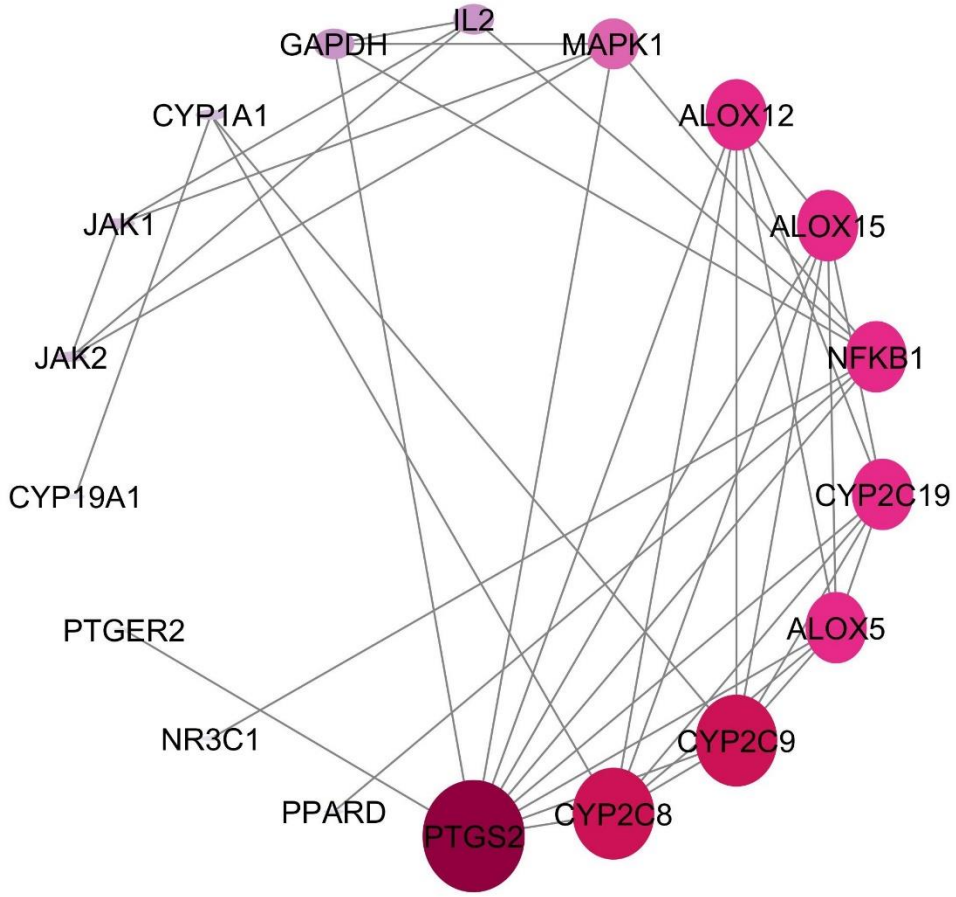


Fig. 4 Degree-sorted potential anti-inflammatory targets of *M. macrantha*

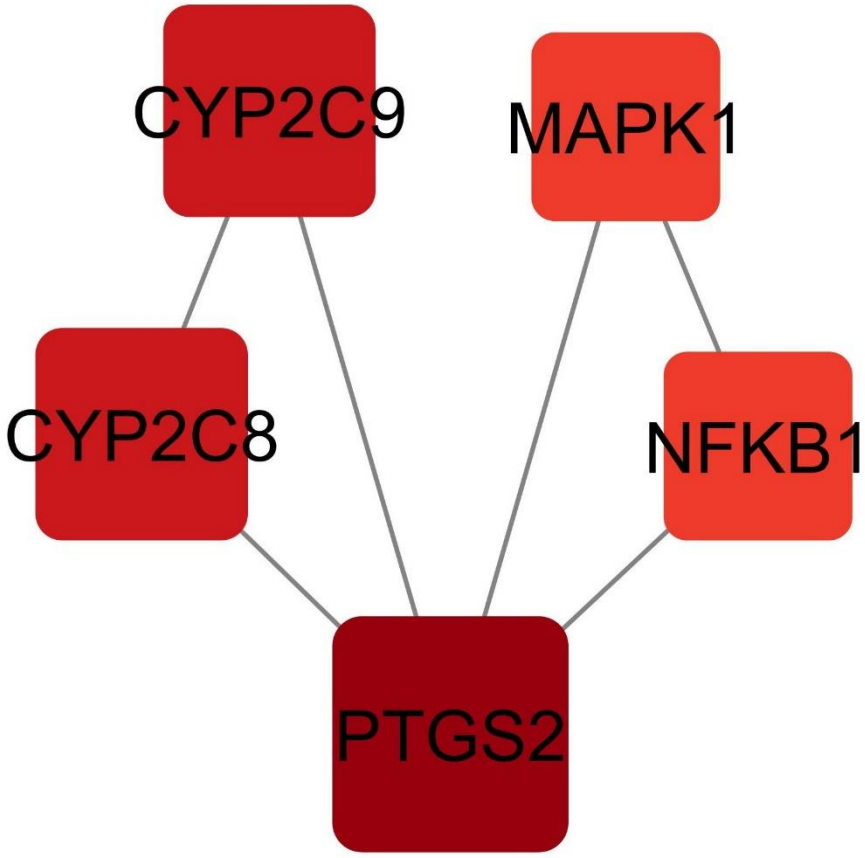


Fig. 5 Central node of the network with the key targets of the PPI network

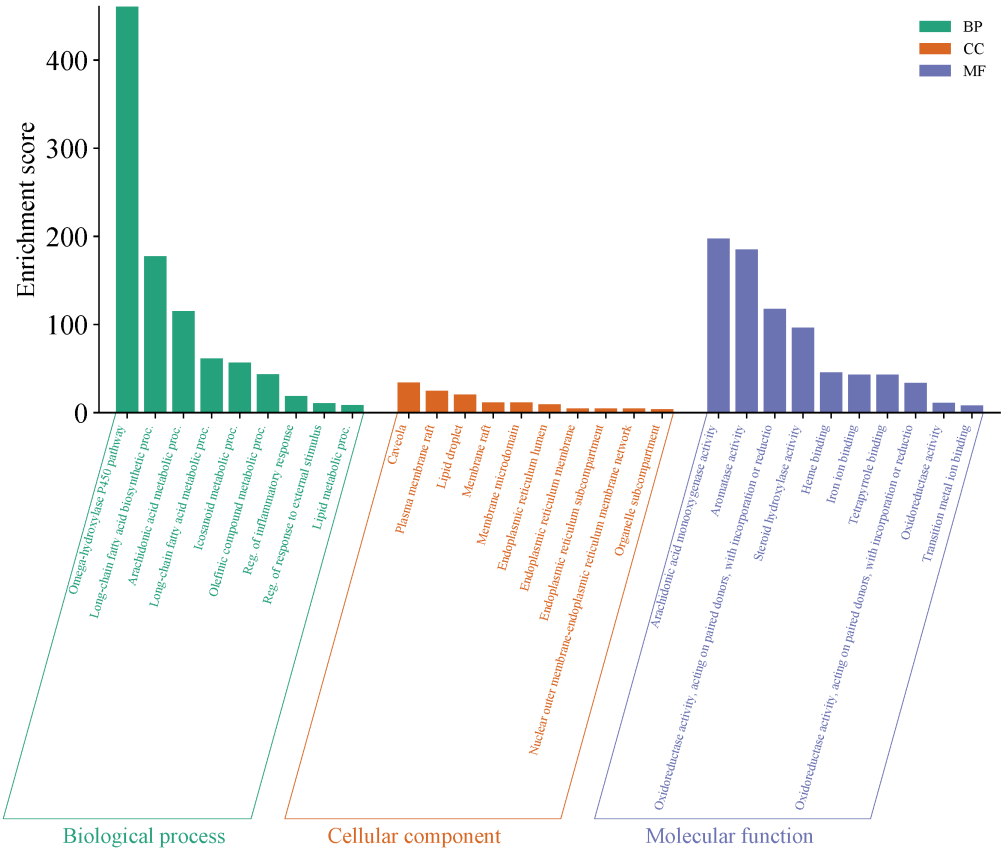


Fig. 6 GO analysis for 23 anti-inflammatory targets of *M. macrantha*

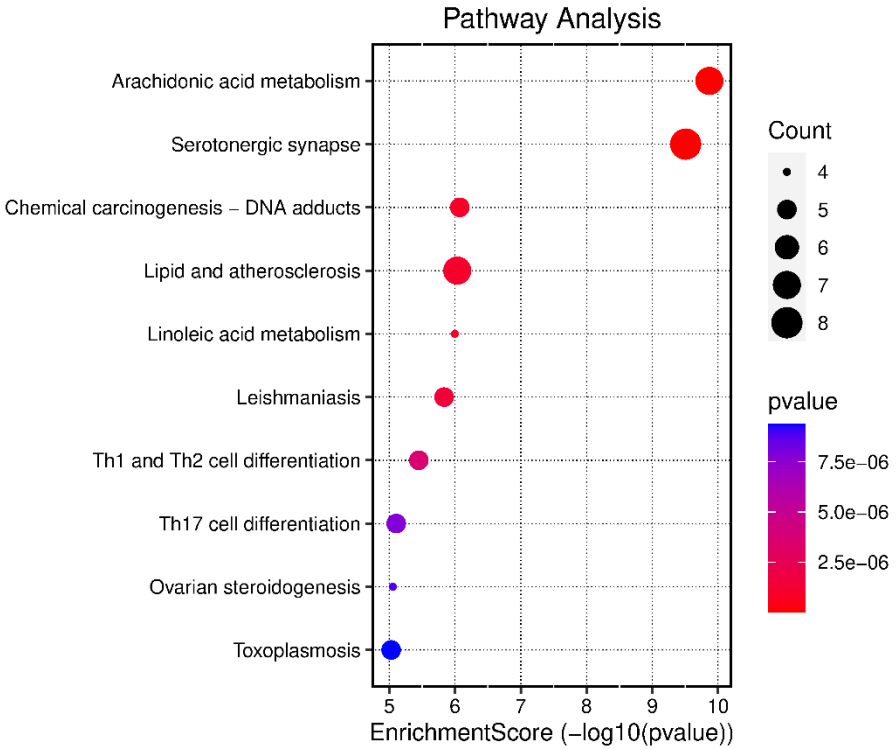


Fig. 7 The Bubble plot graph of 10 most enriched KEGG pathways

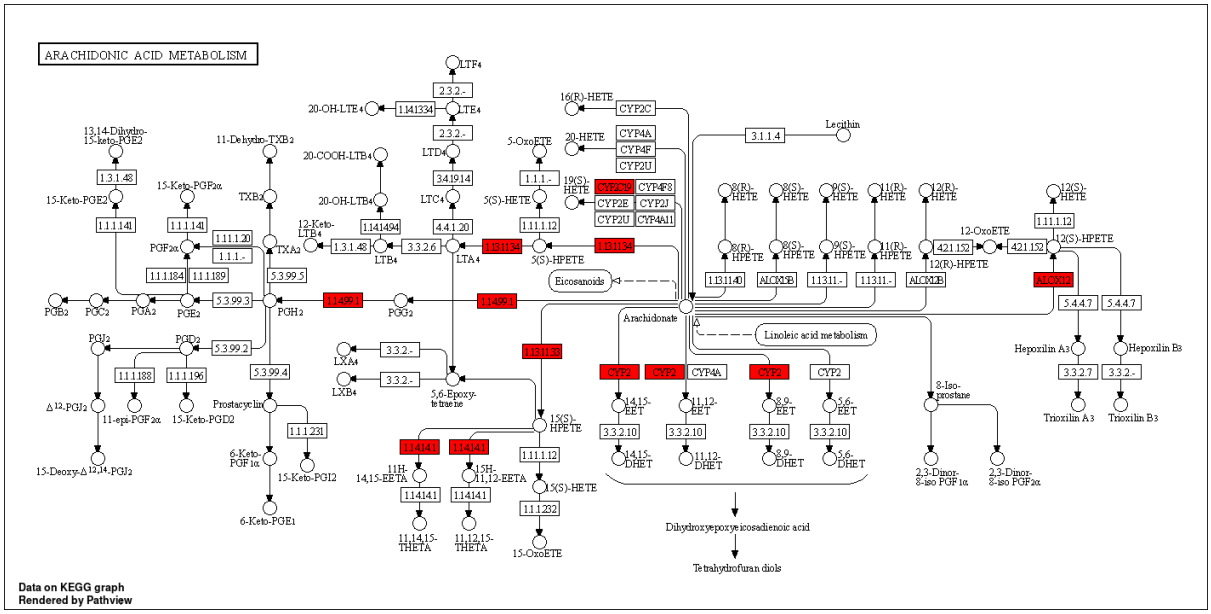
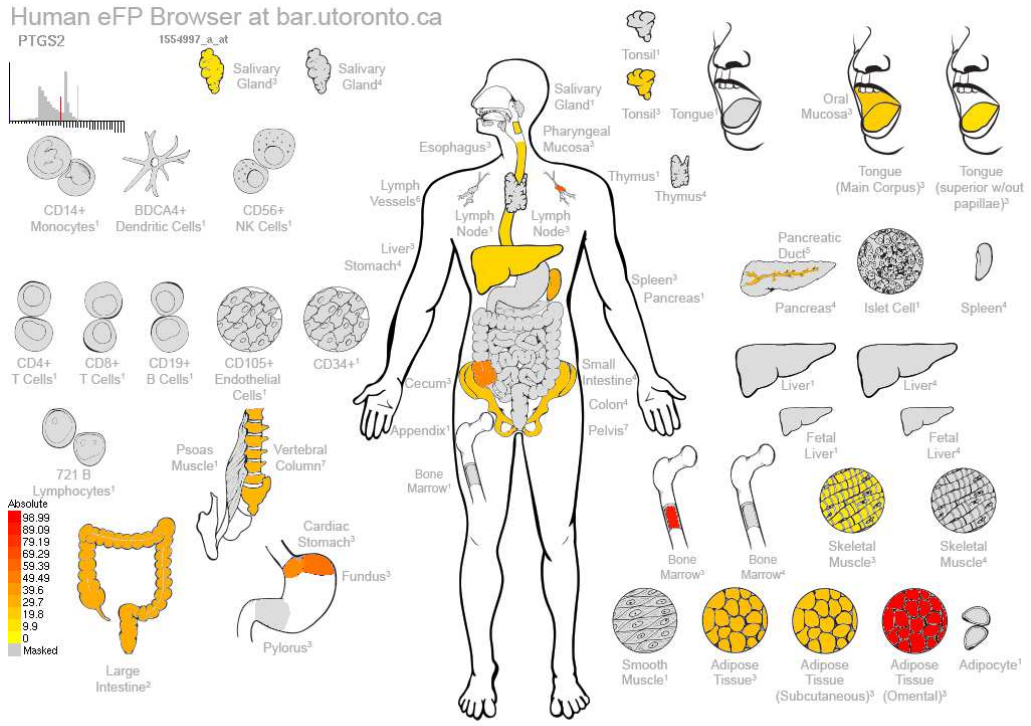
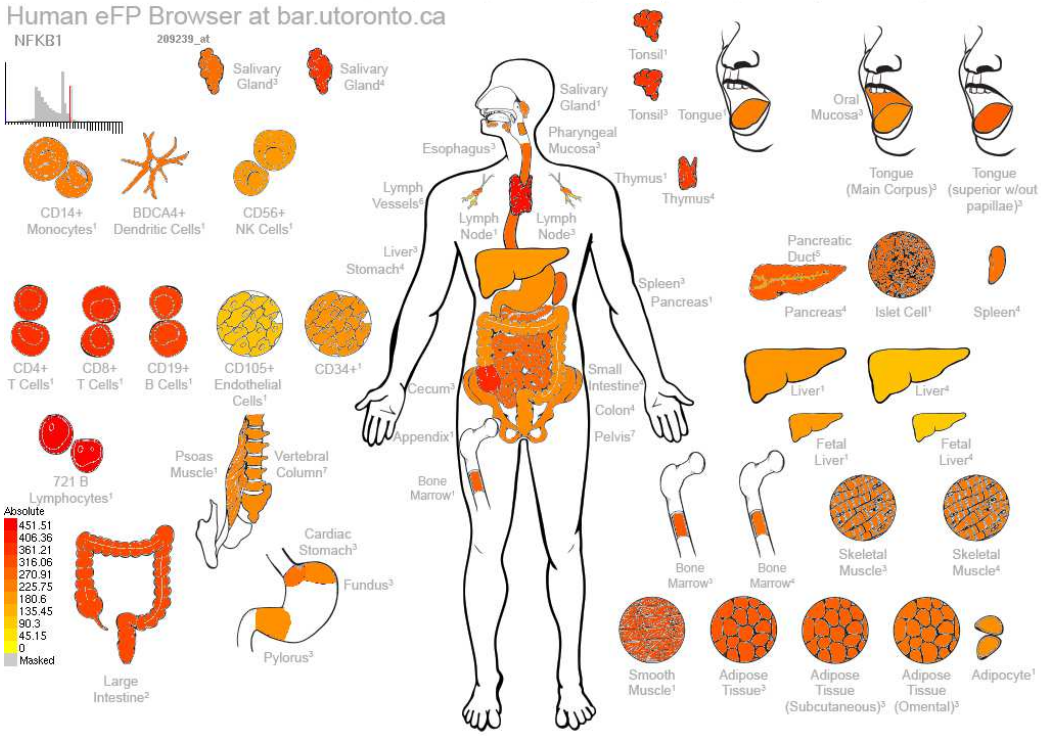


Fig. 8 The highlighted targets of the active constituents of *M. macrantha* in the arachidonic acid metabolism (hsa00590) pathway

A

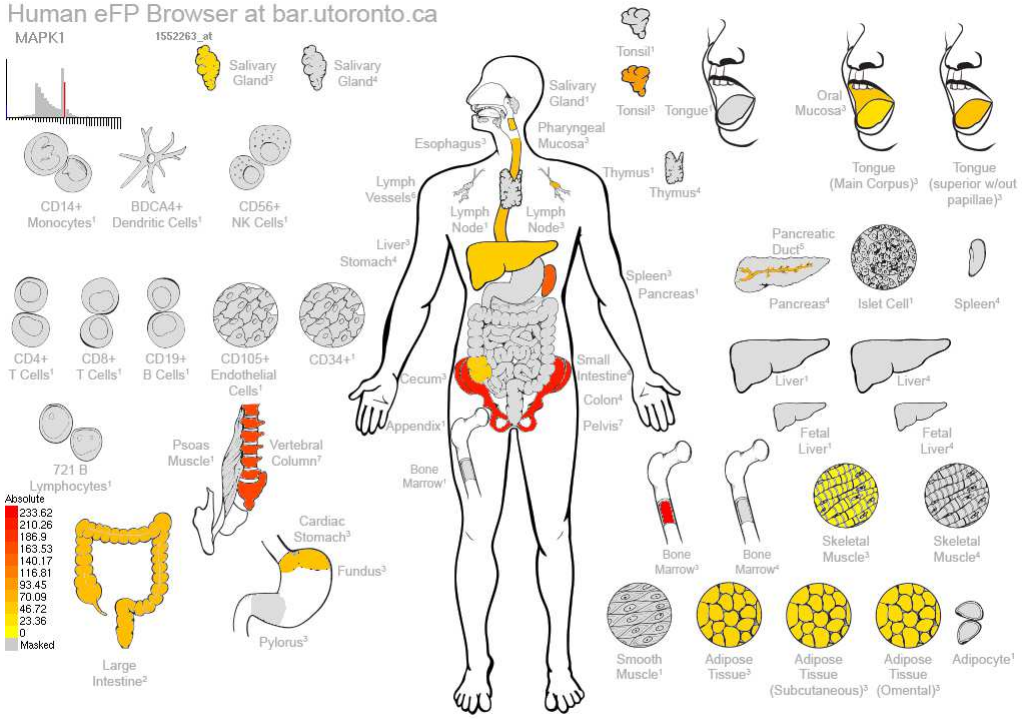


B

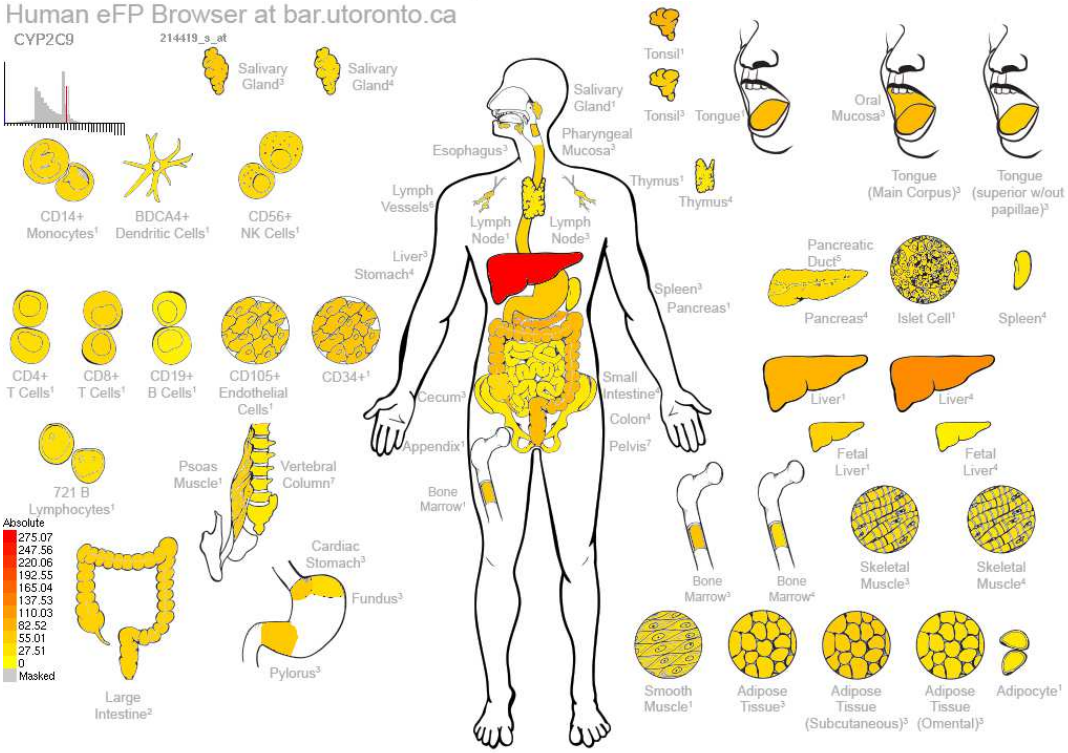


eFP by R. Patel. Images by E. T. Hamanishi. Data from [1]GSE1133; [2]E-GEOD-7307; [3]GSE3526; [4]GSE2361; [5]GSE19650; [6]E-GEOD-6257; [7]E-MEXP-2219.
Data normalized by MAS 5.0 method. TGT value 100.

C



D



eFP by R. Patel. Images by E. T. Hamanishi. Data from [1]GSE1133; [2]E-GEOD-7307; [3]GSE3526; [4]GSE2361; [5]GSE19650; [6]E-GEOD-6257; [7]E-MEXP-2219.
Data normalized by MAS 5.0 method. TGT value 100.

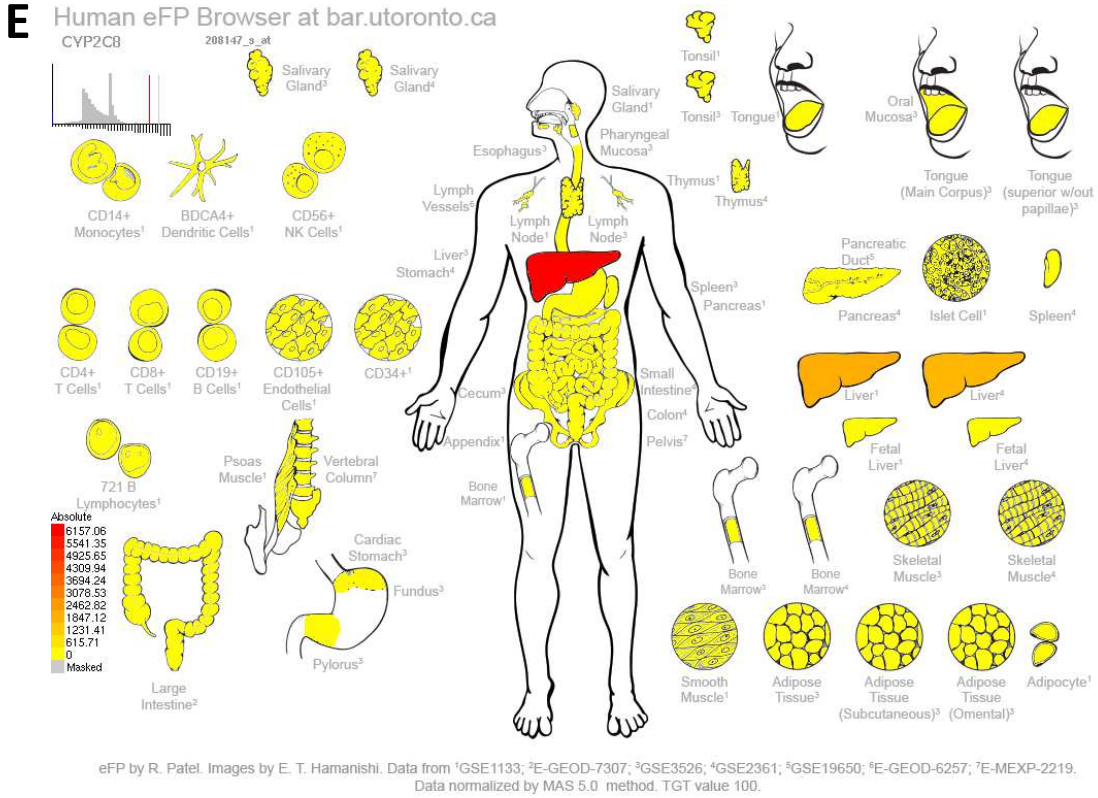


Fig. 9 Analysis for the expression of **A** PTGS2 **B** NFκβ1 **C** MAPK1 **D** CYP2C9 **E** CYP2C8 genes in the digestive, immune and skeletal systems of a normal human

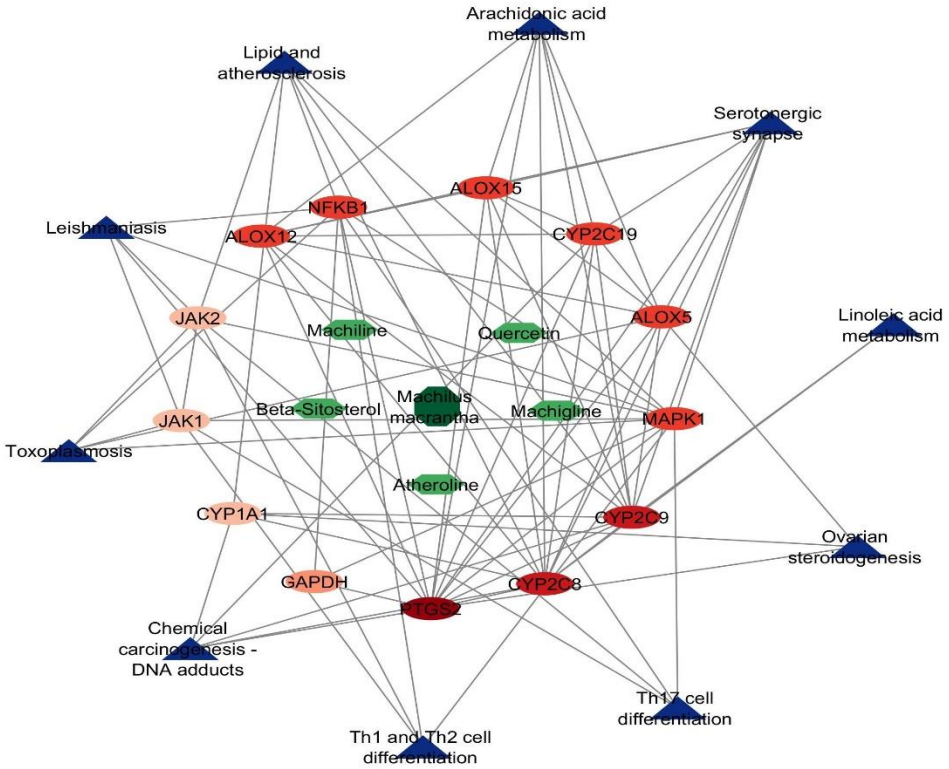
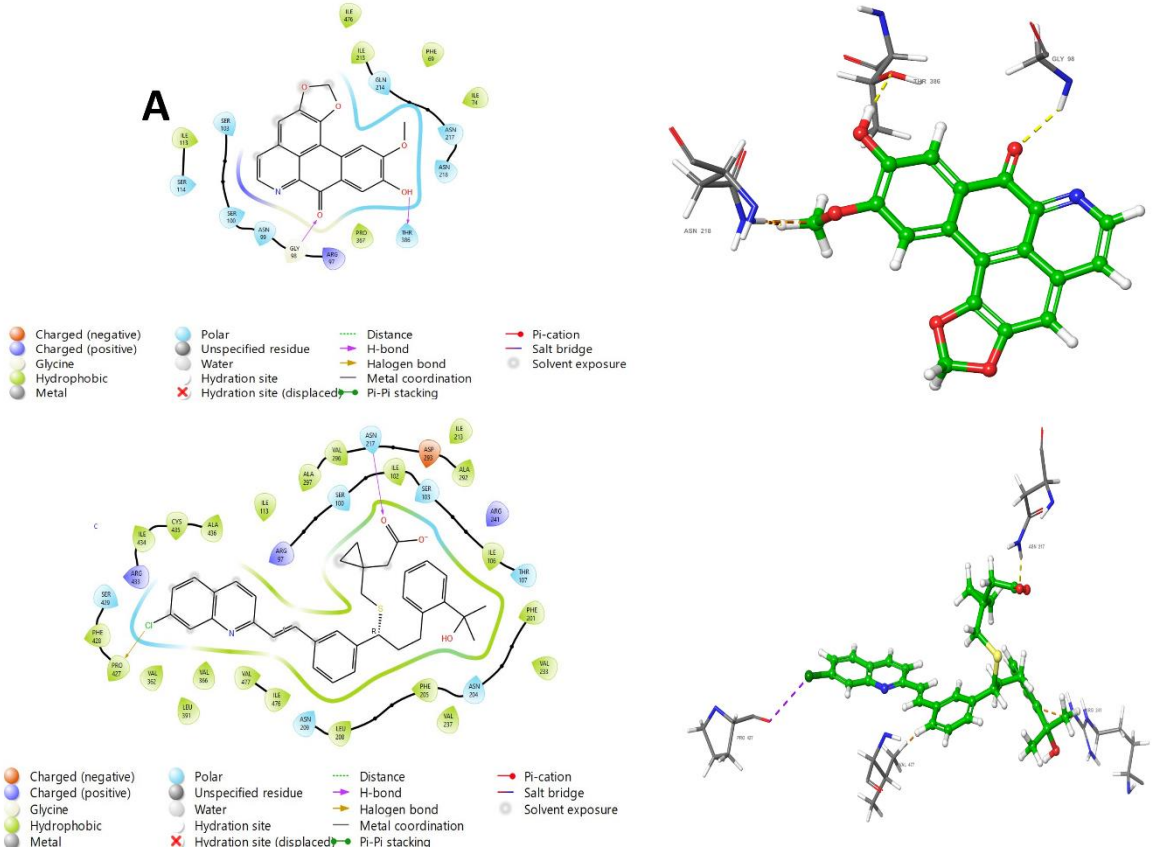
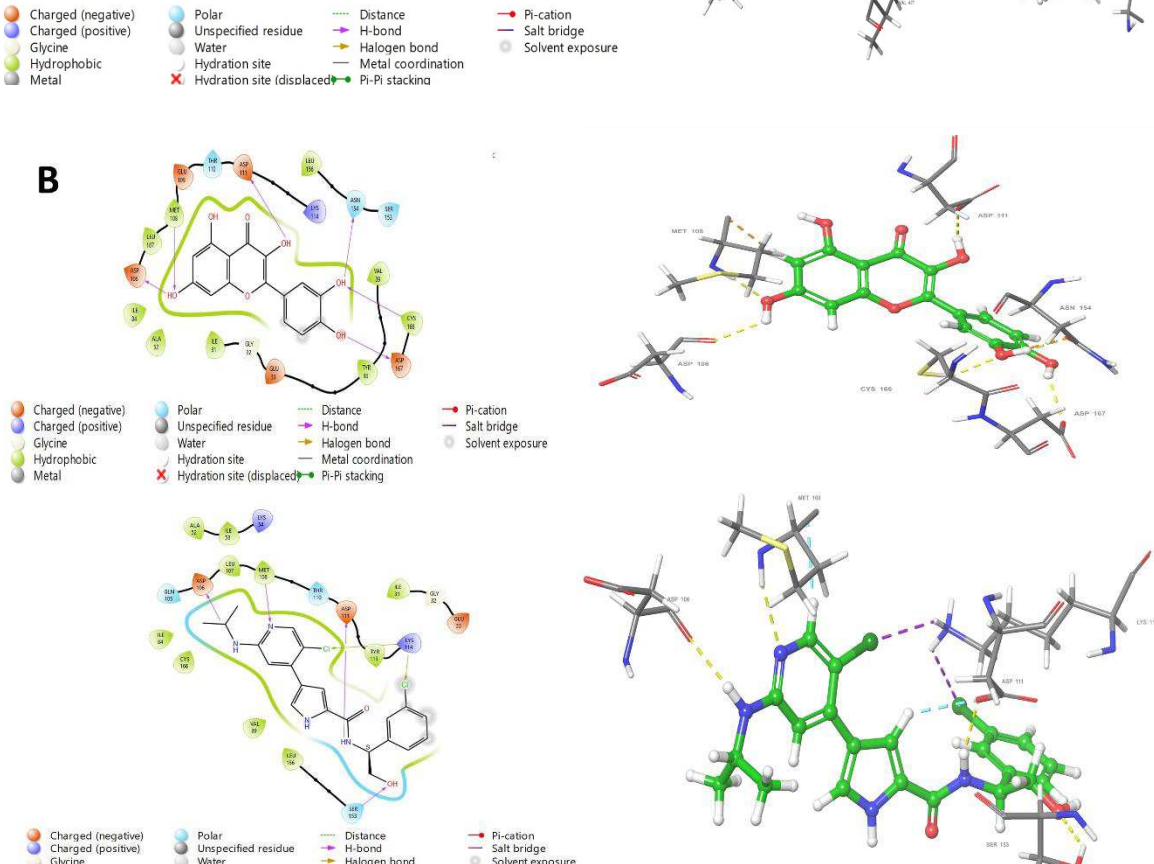
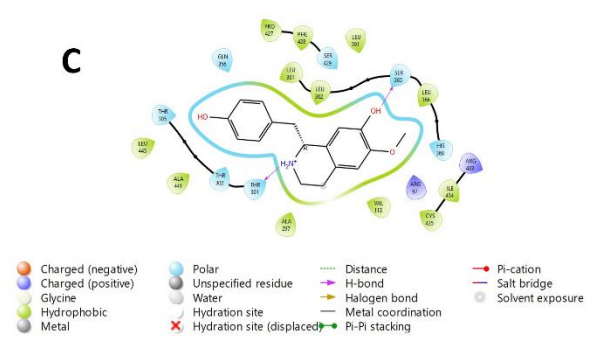


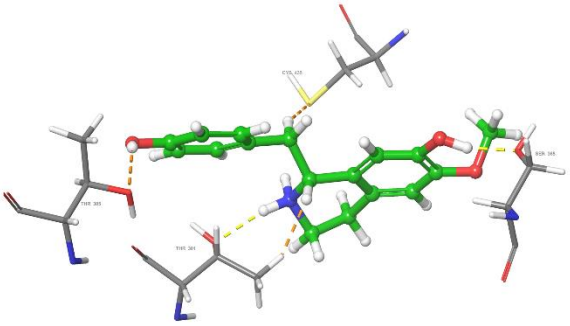
Fig. 10 Ligand-target-pathway interaction network

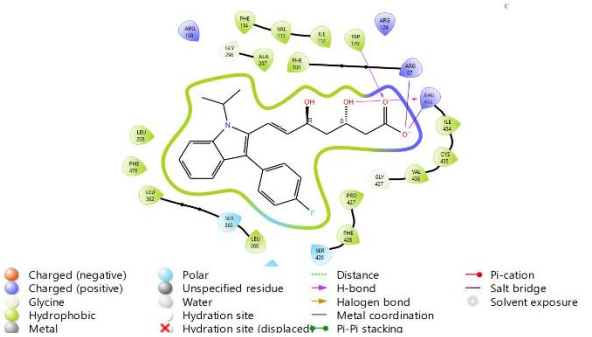

A
Charged (negative)
Charged (positive)
Glycine
Hydrophobic
Metal
Polar
Unspecified residue
Water
Hydration site
Hydration site (displaced)
Distance
H-bond
Halogen bond
Metal coordination
Pi-Pi stacking
Pi-cation
Salt bridge
Solvent exposure

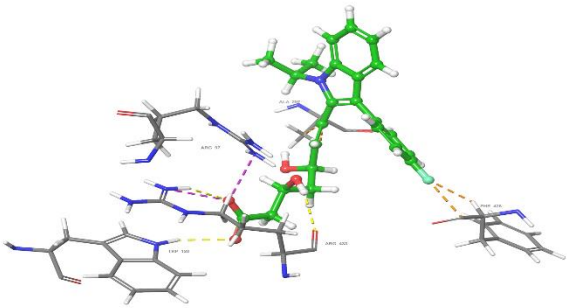

B
Charged (negative)
Charged (positive)
Glycine
Hydrophobic
Metal
Polar
Unspecified residue
Water
Hydration site
Hydration site (displaced)
Distance
H-bond
Halogen bond
Metal coordination
Pi-Pi stacking
Pi-cation
Salt bridge
Solvent exposure

C

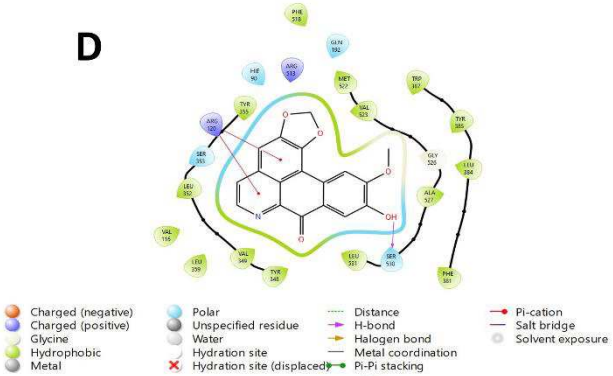

Charged (negative)
Charged (positive)
Glycine
Hydrophobic
Metal
Polar
Unspecified residue
Water
Hydration site
Hydration site (displaced)
Distance
H-bond
Halogen bond
Metal coordination
Pi-Pi stacking
Pi-cation
Salt bridge
Solvent exposure

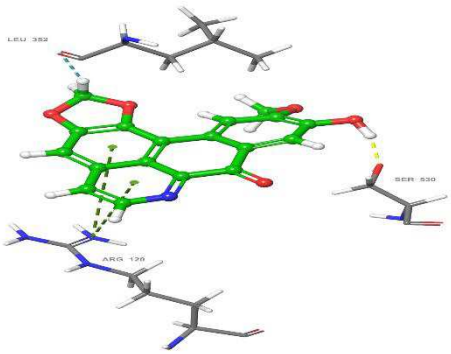


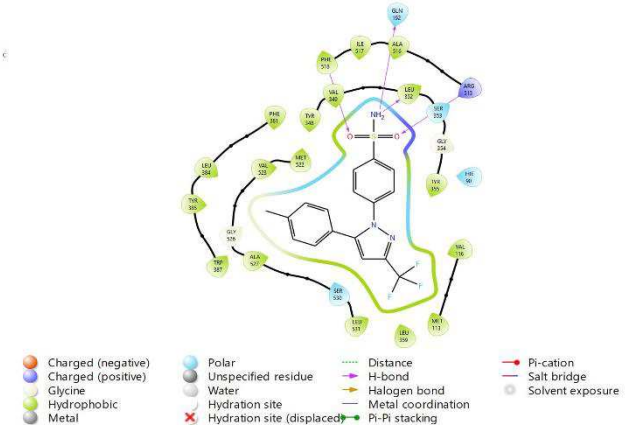

Charged (negative)
Charged (positive)
Glycine
Hydrophobic
Metal
Polar
Unspecified residue
Water
Hydration site
Hydration site (displaced)
Distance
H-bond
Halogen bond
Metal coordination
Pi-Pi stacking
Pi-cation
Salt bridge
Solvent exposure

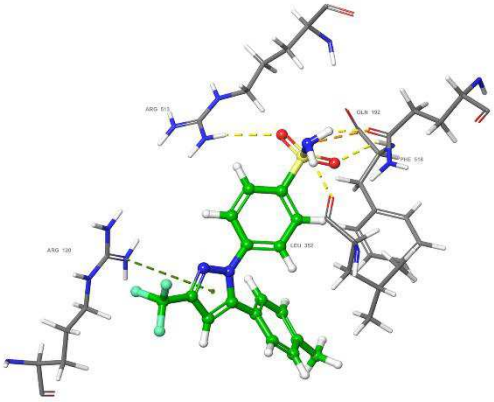


D


Charged (negative)
Charged (positive)
Glycine
Hydrophobic
Metal
Polar
Unspecified residue
Water
Hydration site
Hydration site (displaced)
Distance
H-bond
Halogen bond
Metal coordination
Pi-Pi stacking
Pi-cation
Salt bridge
Solvent exposure


LEU 382
SER 530
ARG 126


Charged (negative)
Charged (positive)
Glycine
Hydrophobic
Metal
Polar
Unspecified residue
Water
Hydration site
Hydration site (displaced)
Distance
H-bond
Halogen bond
Metal coordination
Pi-Pi stacking
Pi-cation
Salt bridge
Solvent exposure


ARG 513
GLN 192
ARG 120
LEU 382

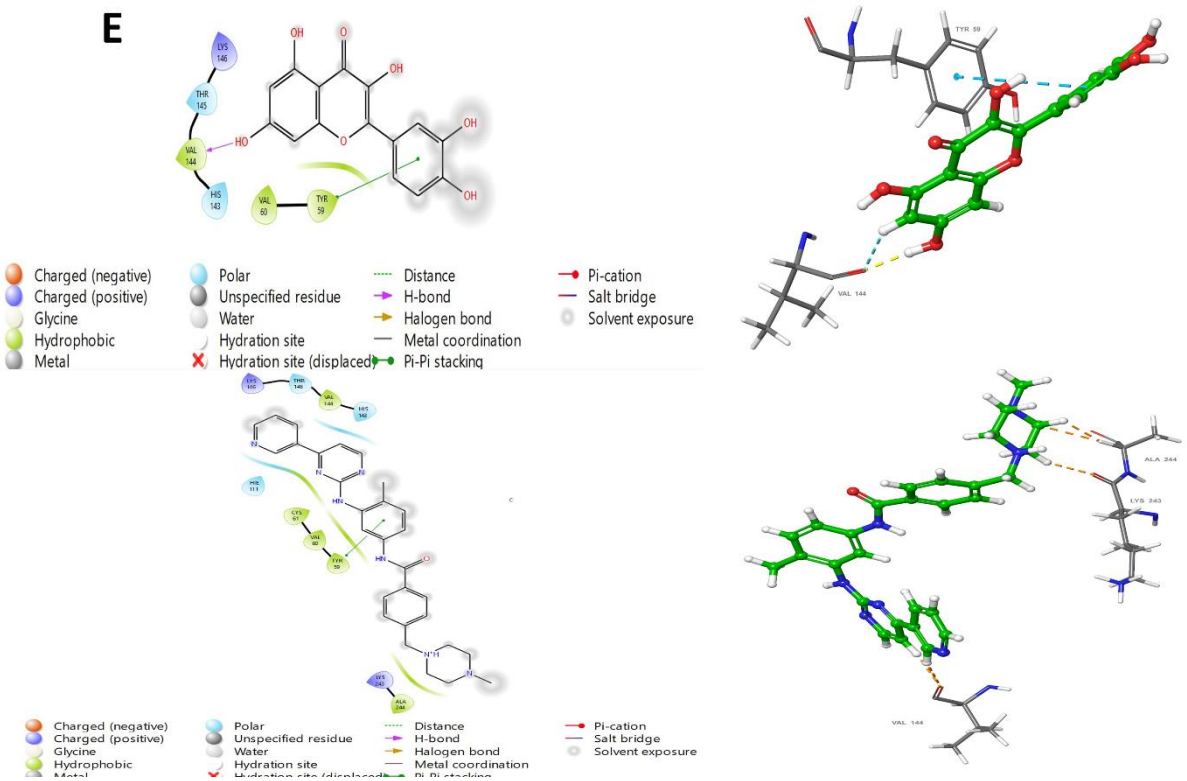


Fig. 11 Results of molecular modelling studies for the main anti-inflammatory targets of *M. macrantha* **A** Montelukast and machigline with 2NNH **B** Quercetin and Ulixertinib with 3W55 **C** Machiline and Fluvastatin with 5K7K **D** Machigline and celecoxib with 5KIR **E** Quercetin and Imatinib with 8TQD

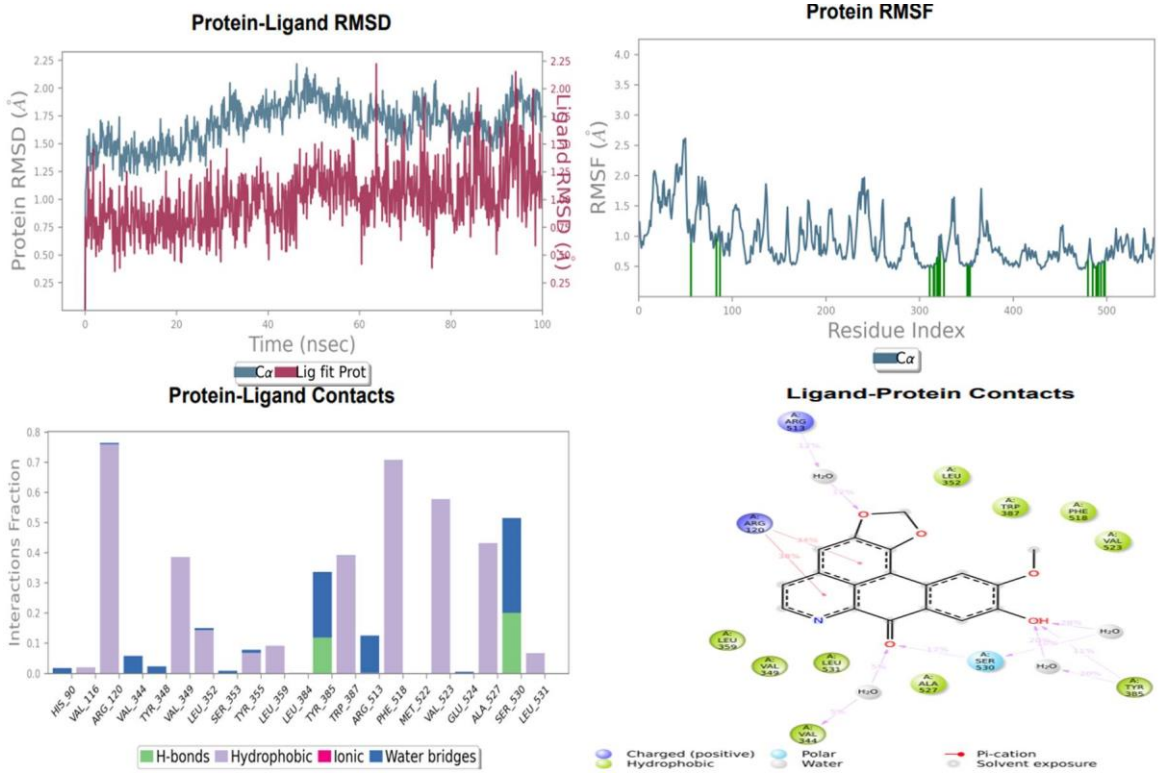


Fig. 12 Protein-ligand RMSD, Protein RMSF, Protein-Ligand contacts and Ligand Protein contacts graphs for Machigline-5KIR complex generated using Desmond software.

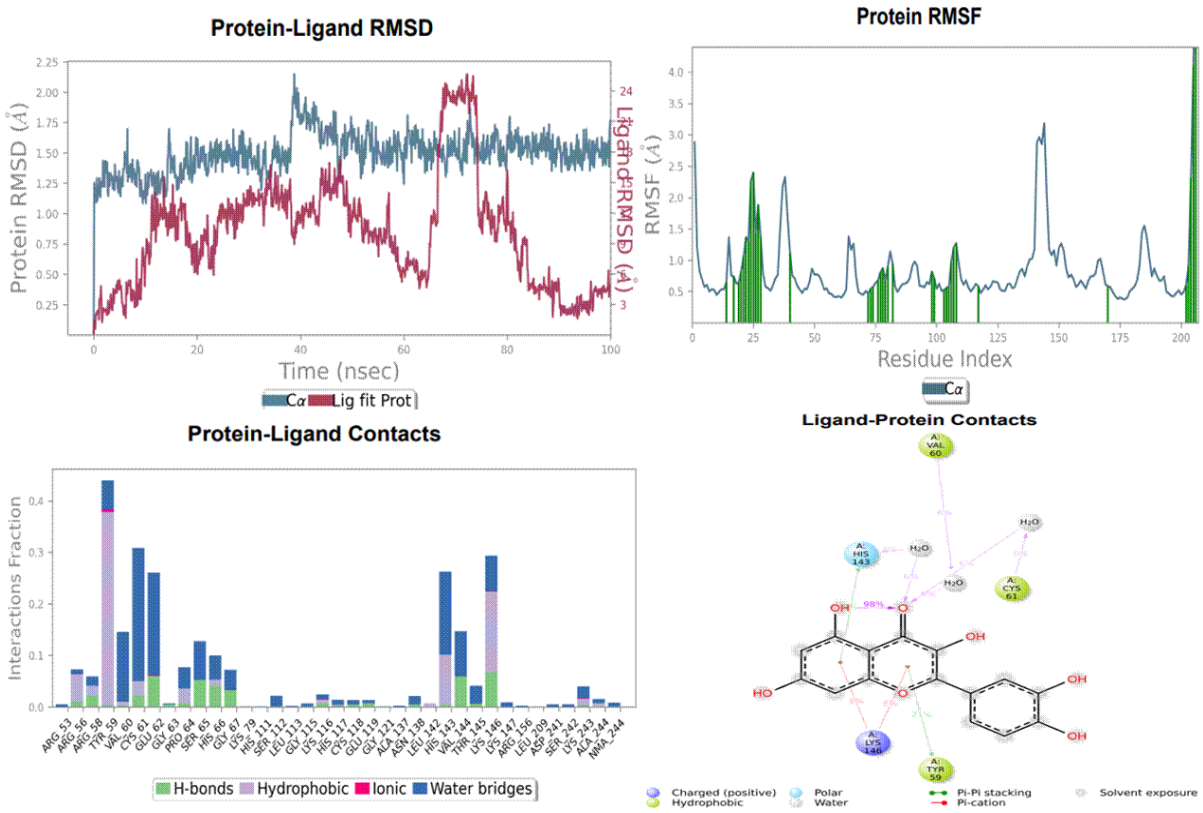


Fig. 13 Protein-ligand RMSD, Protein RMSF, Protein-Ligand contacts and Ligand Protein contacts graphs for Quercitin-8TQD complex generated using Desmond software.

Figure legends

1. Work flow of the study protocol
2. Venn diagram (intersection denotes the major anti-inflammatory targets)
3. PPI interaction diagram
4. Degree-sorted potential anti-inflammatory targets of *M. macrantha*
5. Central node of the network with the key targets of the PPI network
6. GO analysis for 23 anti-inflammatory targets of *M. macrantha*
7. The Bubble plot graph of 10 most enriched KEGG pathways
8. The highlighted targets of the active constituents of *M. macrantha* in the arachidonic acid metabolism (hsa00590) pathway
9. Analysis for the expression of (A): PTGS2 (B): NFκβ1 (C): MAPK1 (D): CYP2C9, and (E): CYP2C8 genes in the digestive, immune and skeletal systems of a normal human
10. Ligand-target-pathway interaction network
11. Results of molecular modelling studies for the main anti-inflammatory targets of M. macrantha (A): Montelukast and machigline with 2NNH (B): Quercetin and Ulixertinib with 3W55 (C): Machiline and Fluvastatin with 5K7K (D): Machigline and celecoxib with 5KIR (E): Quercetin and Imatinib with 8TQD
12. Protein-ligand RMSD, Protein RMSF, Protein-Ligand contacts and Ligand Protein contacts graphs for Machigline-5KIR complex generated using Desmond software.
13. Protein-ligand RMSD, Protein RMSF, Protein-Ligand contacts and Ligand Protein contacts graphs for Quercitin-8TQD complex generated using Desmond software.